A SYNTHESIZED BOUNDARY CONDITION USING ENSEMBLE AVERAGED SURFACE NORMAL IMPEDANCE FOR WAVE-BASED ROOM ACOUSTICS SIMULATIONS

Toru Otsuru
Oita University, Faculty of Engineering, Dannoharu 700, Oita 870-1192, Japan
email: otsuru@oita-u.ac.jp

Reiji Tomiku
Oita University, Faculty of Engineering, Dannoharu 700, Oita 870-1192, Japan

Noriko Okamoto
The University of Kitakyushu, Faculty of Environmental Engineering, Kitakyushu 808-0135, Japan

Saki Yamauchi and Sakura Saigo
Oita University, Graduate School of Engineering, Dannoharu 700, Oita 870-1192, Japan

Wave-based room acoustics simulations have been increasing their importance in various fields of acoustical researches and design-stages. The problem remained, however, is how to model the rooms ’ absorptive boundary conditions. Conventional absorption indices of materials like sound absorption coefficients or normal impedances are not always suit for such a fine method like finite element method, boundary element and so on. To overcome the situation, in previous studies, the authors had proposed the concept and measurement technique of ensemble averaged surface normal impedance of material. Herein, the outline of the concept of ensemble averaged impedance including the measurement technique was summarized, first. Second, several example results of practical measurements were given to exhibit that their uncertainties stay within the range for wave-based simulations to keep their resulting uncertainties less than just noticeable difference. Finally, the results of sound field simulations of realistic rooms are shown to examine the plausibility of the model.

Keywords: finite element method, surface impedance, measurement method, sound absorption

1. Introduction

Recently, wave-based room acoustics simulations like finite element method, boundary element method, and so on, have been intensively used in broad range of the field on acoustics [1, 2, 3]. The authors have been developing a system of large-scale finite element sound field analysis, or LsFE-SFA, and also have presented papers both in time and frequency domains [4, 5, 6, 7, 8]. In the computations of the kind, some reliable impedance data of boundaries are required to assure their accuracy. Then, the authors have also proposed an experimental method to obtain a material's surface normal impedance using ensemble averaging technique, "EA method," with two-micropone [9], as well as with PU-sensor [10]. To obtain normal impedance with more reliability, we also presented a paper on PU-sensor calibration [11].

In this paper, at first, the basis of finite element method to analyze the sound field in a room with dissipative walls is summarized briefly. Next, the outline of EA method is introduced. Then, an example application result of measured impedance by EA method supplied into sound field analysis by LsFE-SFA is given to show the effectiveness of LsFE-SFA supported by EA method.

2. Basis of finite element sound field analysis [4, 6, 7, 8]

The equations to analyze the sound field of a room with dissipative walls are as follows:

$$[K]\{p\} + i\omega[C]\{p\} - \omega^2[M]\{p\} = i\omega\rho v_0\{W\}. \tag{1}$$

Where, $[M]$, $[C]$ and $[K]$ denote acoustic mass, dissipation and stiffness matrices respectively; and $\{p\}$, ρ, ω, u and $\{W\}$ are sound pressure vector, air density, angular frequency, displacement and distribution vector respectively. Assuming that E and to be first and second order derivative with respect to time respectively, the equation in the time domain can be:

$$[M]\{\ddot{p}\} + [C]\{\dot{p}\} + [K]\{p\} = \rho\omega^2 u\{W\}(= \{f\}). \tag{2}$$

With an interpolation (shape) function, $\{N\}$, the acoustic element matrices that construct global matrices in the Eq.(1) are given by

$$[K]_e = \int_e \left(\{\frac{\partial N}{\partial x}\}\{\frac{\partial N}{\partial x}\}^T + \{\frac{\partial N}{\partial y}\}\{\frac{\partial N}{\partial y}\}^T + \{\frac{\partial N}{\partial z}\}\{\frac{\partial N}{\partial z}\}^T \right) dV, \tag{3}$$

$$[M]_e = \frac{1}{c^2}\int_e \{N\}\{N\}^T dV, \tag{4}$$

$$[C]_e = \frac{1}{c}\int_{e'} \frac{1}{z_n}\{N\}\{N\}^T dS. \tag{5}$$

Where c and z_n are sound speed and normal surface impedance respectively, and e' denotes the surface area to be integrated.

In the time domain, we employed Newmark β method to solve the eq. (2) step by step. If $\{p\}_t$, $\{\dot{p}\}_t$ and $\{\ddot{p}\}_t$ at t, are known, then, $\{p\}_{t+\Delta t}$ and $\{\dot{p}\}_{t+\Delta t}$ can be given by

$$\{p\}_{t+\Delta t} = \Big\{ \{p\}_t + \Delta t\{\dot{p}\}_t + (\Delta t)^2(\frac{1}{2} - \beta)\{\ddot{p}\}_t + (\Delta t)^2\beta\{\ddot{p}\}_{t+\Delta t} \Big\}, \tag{6}$$

$$\{\dot{p}\}_{t+\Delta t} = \Big\{ \{\dot{p}\}_t + \Delta t(1-\gamma)\{\ddot{p}\}_t + \Delta t\gamma\{\ddot{p}\}_{t+\Delta t} \Big\}. \tag{7}$$

Here, Δt is time interval between t and $t + \Delta t$, and γ and β are parameters (in the following sections, $\gamma = 1/2$ and $\beta = 1/4$ are assumed). Then, with the Eqs. (6) and (7), we can transform Eq. (2) into:

$$\Big[[M] + \frac{\Delta t}{2}[C] + \beta(\Delta t)^2[K] \Big]\{\ddot{p}\}_{t+\Delta t} = \Big\{ \{f\}_{t+\Delta t} - [C]\{P\} - [K]\{Q\} \Big\}, \tag{8}$$

here,

$$\{P\} = \Big\{ \{\dot{p}\}_t + \frac{\Delta t}{2}\{\ddot{p}\}_t \Big\}, \quad \{Q\} = \Big\{ \{p\}_t + \Delta t\{\dot{p}\}_t + (\frac{1}{2} - \beta)(\Delta t)^2\{\ddot{p}\}_t \Big\}. \tag{9}$$

Thus, $\{\ddot{p}\}_{t+\Delta t}$ can be obtained by solving eq.(10) that is in the form of a linear equation:

$$[A]\{x\} = \{b\}. \tag{10}$$

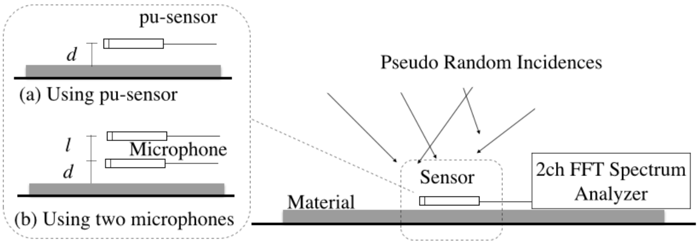

Figure 1: **Schematic diagram of the measurement setup with (a) PU-sensor, and (b) two microphones.**

3. EA method and synthesized boundary condition

3.1 EA method outline [9, 10, 12]

The measurement setup of EA method is depicted in Fig. 1: one with a two-microphone and another with a PU-sensor. In this paper, the latter is used.

If particle velocity and sound pressure are measured at a single point on a material's surface, ensemble averaged surface normal impedance $\langle Z_{\mathrm{n}} \rangle$ and corresponding absorption coefficient $\langle \alpha \rangle$ can be calculated by the following equations:

$$\langle Z_{\mathrm{n}} \rangle = \frac{\langle P_{\mathrm{surf}} \rangle}{\langle U_{\mathrm{n,surf}} \rangle}, \tag{11}$$

$$\langle \alpha \rangle = 1 - \left| \frac{\langle Z_{\mathrm{n}} \rangle - 1}{\langle Z_{\mathrm{n}} \rangle + 1} \right|^2. \tag{12}$$

Here, $U_{n,surf}$ and P_{surf} respectively denote particle velocity normal to the material surface and sound pressure at the material surface in frequency domain. The symbol $\langle x \rangle$ expresses ensemble average of a valuable x. In a practical measurement, ensemble averaged values in the right side of eq. (11) are obtainable from standard outputs of a fast-Fourier-transform (FFT) instrument connected to a PU-sensor, if the sensor is small enough to be placed at the material surface.

In reality, however, an acoustical sensor has a certain size; and the PU-sensor (Microflown, PU Regular) employed in the following investigations has a diameter of half inch. Our former studies revealed both experimentally and computationally that the distance d between PU-sensor and material surface brings no significant difference in measured sound absorption coefficients in case d is less than 13 mm [12]. In the following sections, d is fixed to 10 mm as is genaraly used in our previous studies.

3.2 Synthesized boundary using ensemble averaged impedance

In our previous paper [14], we showed that EA method can provide sound absorption characteristics with less uncertainties that satisfy Vorländer's tentative requirement for room acoustics simulations [13]. The measured value by EA method is ensemble averaged surface normal impedance $\langle Z_{\mathrm{n}} \rangle$ at random incidence. In practical situations, the incidence conditions frequently have certain probability distributions. Even in such cases, $\langle Z_{\mathrm{n}} \rangle$ represents the specific property of the material's absorption as an averaged value over the probability distribution.

In case the material's absorption has no incident-angle-dependency, *e.g.* locally reactive, then $\langle Z_{\mathrm{n}} \rangle$ equals to Z_{n}. In case it has incident-angle-dependency, $\langle Z_{\mathrm{n}} \rangle$ is still rational to represent above mentioned averaged value. It is known that natural noise frequently has the characteristics of white noise and we also showed the availability of ambient noise as sound source in EA method measurement with two-microphone [9].

When an absorptive boundary is model in FEM formulation, eq. (5) shows that Z_{n} needs to represent the absorption around the surface area, not the nodal point itself, to be integrated. Then,

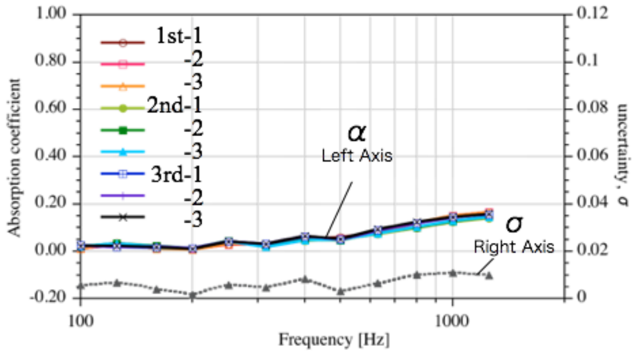

Figure 2: **Sound absorption coefficients (left axis) and included uncertainties (right axis) of a needle felt sheet measured by nine times repeated EA method measurements with a PU-sensor on different three days.**

Figure 3: **Photo of needle felt measured by EA method.**

$\langle Z_{\mathrm{n}} \rangle$ is time and space averaged value and is suit for constructing a synthesized boundary condition of LsFE-SFA.

3.3 Uncertainty of EA method measurement

The tentatively proposed criterion required for an absorption coefficient measurement is "uncertainty (standard deviation) < 0.04." [13] The requirement, however, changes depending on the volume and absorption of the room. So, we have been using the criterion mainly for reference sake.

An example investigation on the uncertainty included in the EA method measurement is shown in Fig. 2. A needle felt with the dimensions of 500 mm × 500 mm × 10 mm (Fig. 3) is laid on the floor of the reverberation room at Oita University. A PU-sensor (PU regular; Microflown Technology) is located at 1 cm above the center of the sheet. Measurements were repeated three times a day on different three days, *i.e.* number of repetition is nine. PU-sensor calibrations were carried out using a standing-wave-tube just before or soon after the sound absorption measurements in the reverberation room. In Fig. 2, considerably small uncertainties are observed throughout the frequency region from 100 Hz to 1250 Hz. We also confirmed similar uncertainties for glass wool, slice form, e.t.c., when appropriate PU-sensor calibration is conducted. [11]

4. Example application for room acoustics simulation

4.1 Analyzed model and measurement settings

To examine the validity of the synthesized boundary condition, both measurements and time domain LsFE-SFA simulations were conducted as below. The sound field in a small room illustrated in Fig. 4 is to be measured and simulated.

The model room is made of acrylic resin with 15 mm thick and is put in the anechoic room of Oita University. As a sound source, a loudspeaker (D1405 driver; Fostex Co.) is attached to a hole at

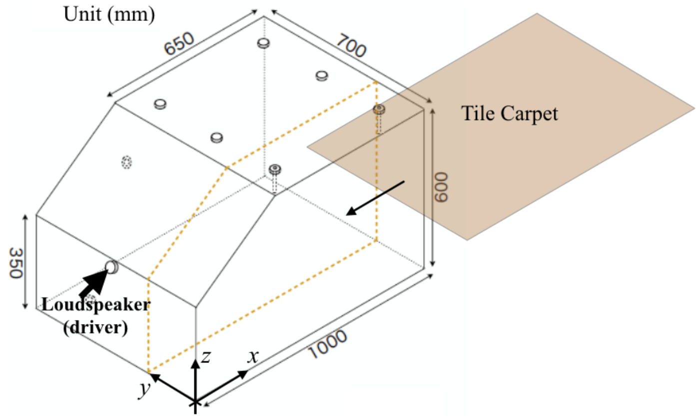

Figure 4: **Small room for impulse response measurement and simulation. (Unit: mm)**

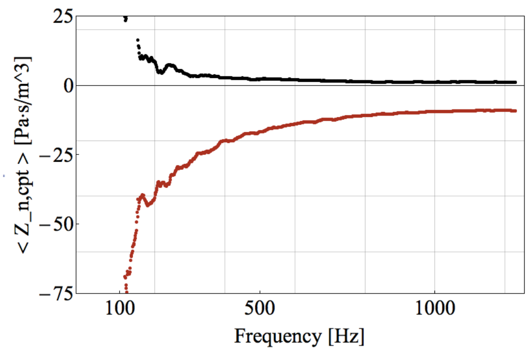

Figure 5: **Real part (Black) and imaginary part (Red) of measured surface normal impedance of Tile Carpet $\langle Z_{\mathrm{n,cpt}} \rangle$ by EA method with PU-sensor.**

(150, 550, 0); and six receiving points are distributed in the model room. Two 1/4 inch microphones (type 4939; B & K) are placed at the receiving points. To realize an absorptive boundary condition, a sheet of tile carpet with 5 mm thick is laid on the floor of the model room. Then, using the swept pulse, impulse responses at the receiving points were measured. Measurements were repeated two times: on the empty condition and on the absorptive condition with the tile carpet.

4.2 Settings for FEM simulations

At first, reverberation times of the empty condition were calculated from above mentioned measured impulse responses using Schroeder integration method and Sabine's equation to obtain the absorption coefficient α_{acr} of acrylic resin. With the value of α_{acr}, acrylic resin's normal impedance value $Z_{\mathrm{n,acr}}$ was calculated assuming that imaginary part of $Z_{\mathrm{n,acr}}$ to be zero.

Then, surface normal impedance of the above mentioned tile carpet $\langle Z_{\mathrm{n,cpt}} \rangle$ was measured by EA method with a PU-sensor in the reverberation room. With the same settings, measurements were repeated three times and measured raw data were averaged over the repetition. Here, to eliminate unnecessary fluctuations, simple moving averaging of 25 data (31.25 Hz) are performed; and the real and imaginary parts of $\langle Z_{\mathrm{n,cpt}} \rangle$ are plotted in Fig. 5.

When a boundary condition is constructed using an impedance value in the frequency domain for LsFE-SFA, frequency dependency of the absorption is modeled straightforwardly. While, when it is constructed in the time domain, an averaged value over a frequency band is necessary to give approximated results of the computation. Hereafter, an example result of LsFE-SFA in the time domain is shown using averaged impedance value over target frequency band.

In the following simulation, we focus our investigation on the frequency range of 1/1 octave band

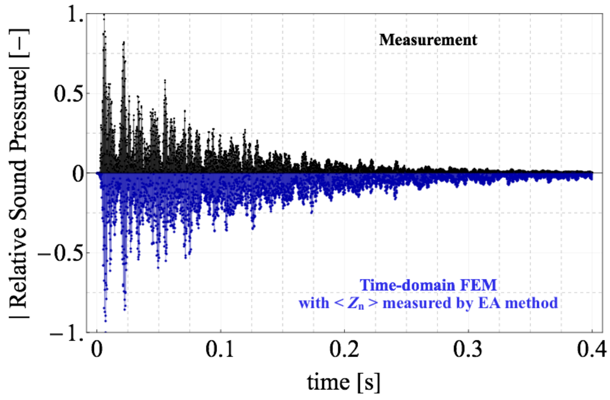

Figure 6: **Comparison of 1/1 octave band pass filtered impulse responses centered at 500 Hz between the results of measurement (Black) and LsFE-SFA simulation in the time domain using $\langle Z_{\mathrm{n,cpt}} \rangle$ (Blue).**

centered at 500 Hz. Then, time swept pulse filtered through the band is given as the external force term in eq. (2). Impedance value is assigned as the mean value over the band.

4.3 Results and discussion

Fig. 6 gives a comparison between measured and computed impulse responses at the receiving point (450, 600, 450) in the model room. In the figure, absolute values of sound pressure are plotted for measurement, while absolute values times (-1) are plotted for simulation.

On the whole, outlines of the impulse responses obtained by measurement and by LsFE-SFA agree well each other. Several peaks around 0.006 s, 0.01 s, 0.02 s, 0.03 s, 0.05 s, 0.06 s, 0.07 s, 0.09 s and so on correspond each other properly between measurement and simulation. While, decay ration of simulation is slower than that of measurement and sound energy stay longer in the simulated sound field than that of measurement. The difference is attributable to under estimation of the averaged absorption of both materials, acrylic resin and tile carpet.

5. Conclusions

With the power of recent PCs, work-stations as well as super-computers, limitations from the computer-hardware side become smaller and FEM sound field analyses, *e.g.* the author's LaFE-SFA, of halls up to 20 kHz have come to be practical. Nonetheless, the problem exists in constructing boundary conditions especially in absorption modelings. To overcome the problem, EA method can be expected to play an important role because it results rather robust surface normal impedance values with small uncertainties. Moreover, the impedance measured by EA method is time and spaced averaged absorptive property of a wall and it is available to construct synthesized boundary condition which suit especially for FEM sound field analyses. The example application shows that measured and simulated impulse responses agree well each other, which reveals the potential of LsFE-SFA with the help of EA method.

Ackowledgements

The authors are grateful to Mr. Tajima for providing excellent technical support continuously. We also thank Mr. Takenaga for contributing to this paper as an undergraduate student. This work was partly supported by JSPS KAKENHI Grant Number 16H04465.

REFERENCES

1. Craggs, A. "An acoustic finite element approach for studying boundary flexibility and sound transmission between irregular enclosures." *J. Sound Vib.* 30.3 (1973): 343-357.
2. Sakuma, T., Yosuke Y.. "Fast multipole boundary element method for large-scale steady-state sound field analysis. Part I: setup and validation." *Acta Acustica united with Acustica* 88.4 (2002): 513-525.
3. Sakamoto, S., "Phase-error analysis of high-order finite difference time domain scheme and its influence on calculation results of impulse response in closed sound field." *Acoust. Sci. & Tec.* 28.5 (2007): 295-309.
4. Otsuru, T., Fujii, K. "Finite elemental analysis of sound fields in rooms with sound absorbing materials," *Proc. INTER-NOISE & NOISE-CON 1994*, 2011-2014 (1994).
5. Otsuru, T., R. Tomiku. "Basic Characteristics and Accuracy of Acoustic Finite Element Using Spline Function in the Applications onto Finite Element Sound Field Analysis." *J. Acoust. Soc. Jpn (E)* (2000): 87-96. http://doi.org/10.1250/ast.21.87
6. Tomiku, R., Otsuru, T., Takahashi. Y., "Finite element sound field analysis of diffuseness in reverberation rooms." *J. Asian Archi. & build. eng.* 1 (2) (2002): 2_33-39. http://doi.org/10.3130/jaabe.1.2_33
7. Okamoto, N., Tomiku, R., Otsuru, T., Yasuda, Y. "Numerical analysis of large-scale sound fields using iterative methods part II: application of Krylov subspace methods to finite element analysis." *J. Comput. Acoust.* 15.04 (2007): 473-493. DOI: http://dx.doi.org/10.1142/S0218396X07003512
8. Okuzono, T., Otsuru, T., Tomiku, R., Okamoto, N., "Fundamental accuracy of time domain finite element method for sound-field analysis of rooms." *Appl. Acoust.* 71.10 (2010): 940-946. http://dx.doi.org/10.1016/j.apacoust.2010.06.004
9. Takahashi, Y., Otsuru, T., Tomiku, R., "In situ measurements of surface impedance and absorption coefficients of porous materials using two microphones and ambient noise," *Appl. Acoust.* 66, 845-865 (2005). doi: 10.1016/j.apacoust.2004.11.004
10. Otsuru, T., Tomiku, R., Din, N. B. C., Okamoto, N., Murakami, M., "Ensemble averaged surface normal impedance of material using an in-situ technique: Preliminary study using boundary element method," *J. Acoust. Soc. Am.* 125 (6) 3784-3791 (2009). DOI: 10.1121/1.3125327
11. Otsuru, T., Tomiku,R., Okamoto, N., Yamauchi, S., "Sound absorption deviation measured using pressure - velocity sensors by ensemble averaging technique under different relative humidity conditions," *Appl. Acoust.* 122, 121 - 127 (2017). DOI: 10.1016/j.apacoust.2017.02.015
12. Din, N. B. C., Otsuru, T., Tomiku, R., Okamoto, N., Asniawaty, K., "Measurement method with a pressure - velocity sensor for measuring surface normal impedance of materials using ensemble averaging: Comparison with other methods and its geometrical configuration," *Acoust. Sci. & Tech.*, 33, 86-95 (2012). DOI: 10.1250/ast.33.86
13. Vorländer, M., "Computer simulations in room acoustics: Concepts and uncertainties," *J. Acoust. Soc. Am.*, 133, 1203-1213 (2013).
14. Otsuru, T., Tomiku, R., Okamoto, N., Ueda, E., "An discussion on the uncertainty of absorption characteristics measured by ensemble averaging technique for room acoustics simulations," *Proc. ICA2016*, CD-ROM (2016).
15. Din, N. B. C., Otsuru, T., Tomiku, R., Okamoto, N., Asniawaty, K., "Reproducibility and applicability of ensemble averaged surface normal impedance of materials using an in-situ technique," *Acoust. Austr.*, 41, 207-212 (2013).